Alteration of Ca^{2+} Dependence of Neurotransmitter Release by Disruption of Ca^{2+} Channel/Syntaxin Interaction

Jens Rettig,[1] Christian Heinemann,[1] Uri Ashery,[1] Zu-Hang Sheng,[2] Charles T. Yokoyama,[2] William A. Catterall,[2] and Erwin Neher[1]

[1]*Department of Membrane Biophysics, Max-Planck-Institute for Biophysical Chemistry, 37077 Göttingen, Germany, and* [2]*Department of Pharmacology, University of Washington, Seattle, Washington 98195-7280*

Presynaptic N-type calcium channels interact with syntaxin and synaptosome-associated protein of 25 kDa (SNAP-25) through a binding site in the intracellular loop connecting domains II and III of the α_1 subunit. This binding region was loaded into embryonic spinal neurons of *Xenopus* by early blastomere injection. After culturing, synaptic transmission of peptide-loaded and control cells was compared by measuring postsynaptic responses under different external Ca^{2+} concentrations. The relative transmitter release of injected neurons was reduced by ~25% at physiological Ca^{2+} concentration, whereas injection of the corresponding region of the L-type Ca^{2+} channel had virtually no effect. When applied to a theoretical model, these results imply that 70% of the formerly linked vesicles have been uncoupled after action of the peptide. Our data suggest that severing the physical interaction between presynaptic calcium channels and synaptic proteins will not prevent synaptic transmission at this synapse but will make it less efficient by shifting its Ca^{2+} dependence to higher values.

Key words: neuromuscular junction; Ca^{2+} dependence; synaptic transmission; calcium channel; synprint; syntaxin

Classic studies by Fatt and Katz (1951) at the frog neuromuscular junction revealed that Ca^{2+} influx into the presynaptic terminal provides the trigger for fast synaptic transmission in the vertebrate CNS. Calcium ions enter the synaptic terminal through voltage-gated calcium channels, which are clustered at specialized regions called active zones (Heuser and Reese, 1981; Robitaille et al., 1990). The release of neurotransmitter molecules is steeply dependent on the external calcium concentration $[Ca^{2+}]_e$. Dodge and Rahamimoff (1967) estimated that the probability of acetylcholine release at the frog neuromuscular junction increases as the fourth power of $[Ca^{2+}]_e$.

The delay between Ca^{2+} influx and fusion of synaptic vesicles is estimated to be in the range of 200–700 μsec (Llinas et al., 1981; Borst and Sakmann, 1996; Yazejian et al., 1997), leading to the suggestion that there might be a physical link between presynaptic channels and proteins of the docking and fusion machinery. Indeed, coimmunoprecipitation studies indicated a close association between ω-conotoxin GVIA-sensitive N-type calcium channels and syntaxin, a 35 kDa protein anchored by its C terminus in the presynaptic membrane and a member of the synaptic core complex (Bennett et al., 1992; Yoshida et al., 1992). An 87 amino acid region from the cytoplasmic loop between homologous repeats II and III ($L_{II\text{-}III}$) of the channel is responsible for binding to syntaxin 1A (Sheng et al., 1994). A peptide containing this synaptic protein interaction (synprint) site also blocks binding of native N-type channels to syntaxin and interacts with synaptosome-associated protein of 25 kDa (SNAP-25) (Oyler et al., 1989), another presynaptic protein involved in docking and fusion of synaptic vesicles. Binding of the peptide to syntaxin and SNAP-25 occurs in a Ca^{2+}-dependent manner, being maximal in the range of 10–30 μM $[Ca^{2+}]$ (Sheng et al., 1996), near the calcium threshold for secretion (for review, see Burgoyne and Morgan, 1995). Recently, it has been shown that introduction of synprint peptide into presynaptic superior cervical ganglion neurons reversibly inhibits synaptic transmission (Mochida et al., 1996), underscoring the physiological significance of this interaction. This inhibition might be attributable to either interference with the secretory machinery or changes in the calcium dependence of transmission as the vesicle is separated from the calcium channel.

To learn about the effect of synprint peptide on the calcium dependence of synaptic transmission, we injected the purified syntaxin binding site of N-type Ca^{2+} channels into one of the early blastomeres of *Xenopus laevis*. Nerve–muscle cocultures obtained from developing *Xenopus* embryos provide a powerful system for the study of synaptic transmission. Synaptic transmission in these cultured neurons is mainly dependent on N-type Ca^{2+} channels (Yazejian et al., 1997), thus making it an ideal preparation for studying the possible interaction of the N-type channels with proteins of the synaptic core complex. During the first days of development, the embryos undergo cell divisions without substantial growth. Injection of macromolecules into early blastomeres therefore leads to efficient loading of all progeny cells, including spinal cord neurons and muscle cells. The effect of the injected macromolecules on synaptic transmission can be assayed at neuromuscular junctions developed by these cells in culture (Tabti and Poo, 1991), and the presynaptic calcium concentration can be monitored with fluorescent indicators. Our results show that synprint peptides reduce the calcium sensitivity

Received May 9, 1997; revised June 17, 1997; accepted June 20, 1997.

This work was supported in part by Grants of the Deutsche Forschungsgemeinschaft (J.R.), a predoctoral fellowship from Boehringer Ingelheim Fonds (C.H.), a postdoctoral Feodor Lynen-Minerva fellowship (U.A.), research Grant NS 22625 from National Institutes of Health (W.A.C.), a postdoctoral fellowship of the National Institute of Mental Health (Z.-H.S.), and a predoctoral fellowship from National Institutes of Health Training Grant T32 GM07108 (C.T.Y.). We thank Dr. Alan Grinnell and members of his laboratory for their kind hospitality and advice.

J.R., C.H., and U.A. contributed equally to this work.

Correspondence should be addressed to Dr. E. Neher at the above address.

Dr. Sheng's present address: Synaptic Function Unit, National Institutes of Health, Bethesda, MD 20892.

of synaptic transmission and support a model in which the synprint peptides increase the distance between docked vesicles and calcium channels.

MATERIALS AND METHODS

Preparation of nerve–muscle cocultures. Xenopus nerve–muscle cocultures were prepared from the neural tube and associated myotomal tissue of stage 20–22 embryos as described (Tabti and Poo, 1991). After dissociation in Ca^{2+}–Mg^{2+}-free solution (125 mM NaCl, 2 mM KCl, 1.2 mM EDTA, 5 mM HEPES, pH 7.6), cells were plated on glass coverslips pretreated for ~60 min with ECL (entactin, collagen, and laminin; Upstate Biotechnologies, Lake Placid, NY) and grown for ~24 hr at 22°C. The culture medium consisted of 70% Leibovitz L-15 supplemented with GMS-X and antibiotics (all components from Life Technologies, Gaithersburg, MD). All electrophysiological experiments were performed 1 d after plating.

Peptide injection and immunoblot analysis. Recombinant His-fusion proteins containing the syntaxin/SNAP-25 binding site of N-type Ca^{2+} channel ($L_{II\text{-}III}$ 718–963) and, as a negative control, the corresponding region of the L-type calcium channel ($L_{II\text{-}III}$ 670–800), were purified as described (Mochida et al., 1996) and concentrated to a final concentration of 1 mg/ml. Peptides were mixed 1:1 with rhodamine-dextran (molecular weight 10,000; 10 mg/ml) (Molecular Probes, Eugene, OR), and ~10 nl of that mixture was injected into one blastomere of embryos at the two- to four-cell stage by pressure injection (Microinjector 5242) (Eppendorf, Hamburg, Germany). For Western blotting, embryos at various stages were collected and homogenized by trituration through Eppendorf tips with 20 μl of extraction buffer (100 mM KCl, 0.1 mM $CaCl_2$, 1 mM $MgCl_2$, 10 mM HEPES, pH 7.7). After centrifugation (14,000 rpm, 10 min), the supernatant of one embryo was loaded onto each lane, separated by SDS-PAGE, and transferred overnight to nitrocellulose (0.2 μm) (Schleicher & Schuell, Dassel, Germany). Immunoblot analysis was performed with Anti-T7.Tag monoclonal antibody (1:10,000) (Novagen, Madison, WI), and the immunoreactive bands were visualized by enhanced chemoluminescence (ECL system) (Amersham, Arlington Heights, IL).

Electrophysiological recordings. Before recording, spinal neurons were examined for rhodamine fluorescence (see optical setup for details). Fluorescent nerve cells were considered peptide-positive. Synaptic currents were recorded from innervated muscle cells in the whole-cell configuration using a combination of EPC-9 and EPC-7/EPC-8 amplifiers driven by the Pulse v8.06 software package (Heka Elektronik, Lambrecht, Germany). The pipette solution for the muscle cells contained 107 mM CsCl, 1 mM $MgCl_2$, 1 mM NaCl, 10 mM EGTA, 10 mM HEPES, pH 7.3. The bath solution contained normal frog Ringer's solution (116 mM NaCl, 2 mM KCl, 1 mM $MgCl_2$, 5 mM HEPES, pH 7.3), with varying calcium concentrations (ranging from 0.3 to 10 mM) as indicated in the figures. Solutions were changed by rapid perfusion with an estimated exchange rate of 2–4 ml/min, the bath volume being 1 ml. To keep approximately the same external divalent cation concentrations, external magnesium concentrations were 2.5, 2.3, and 1.8 mM for 0.3, 0.5, and 1 mM $[Ca^{2+}]_e$, respectively. For 1.8 and 10 mM $[Ca^{2+}]_e$, the external magnesium concentration was kept at 1 mM. The muscle cells were routinely clamped at −50 mV holding potential. A 10 msec test pulse to −60 mV was given before each EPSC sweep to estimate the series resistance for later offline series resistance compensation. Action potentials were routinely elicited on external stimulation (0.3–0.5 msec, 0.2–2 μA) of the nerve cell soma, with frequencies between 0.2 and 1.0 Hz. In the case of fura-2 experiments, the whole-cell configuration was established on the soma of the nerve cell. The nerve cell was held at a potential between −45 and −70 mV in the current clamp mode. Action potentials were elicited every 1–5 sec or as a train of 10 action potentials (20 Hz) with 2 msec current injections of 700–900 pA. The pipette was filled with 114 mM potassium gluconate, 10 mM KCl, 1 mM NaCl, 1 mM $MgCl_2$, 10 mM HEPES, 2 mM MgATP, 0.3 mM GTP, 100 μM fura-2, pH 7.3.

Data analysis. Amplitudes of EPSC were analyzed with locally written software in IGOR (WaveMetrix, Lake Oswego, Oregon). Synaptic currents were counted as evoked currents when they occurred in a 6 msec time window after the stimulus. Because of the large EPSC amplitudes (up to 10 nA), there was sometimes a significant clamp error in our measurements. The series resistance before each EPSC was estimated from the peak of the capacitive current during the test pulse. We corrected the EPSC amplitudes assuming a linear *I–V* relation and a reversal potential of +2 mV (as measured independently). Experiments with clamp errors larger than 30 mV were excluded from further analysis.

Model calculations. Equilibrium calculations for the Ca^{2+} dependence of transmitter release were also performed in IGOR (WaveMetrix). We used a model scheme with four sequential Ca^{2+} binding steps similar to those used to describe the Ca^{2+} dependence of secretion in neuroendocrine cells and bipolar nerve terminals (Heinemann et al., 1994; Heidelberger et al., 1994). The equilibrium Ca^{2+} binding is described in matrix notation by:

$$\begin{pmatrix} 1 & 1 & 1 & 1 & 1 \\ -4\alpha X & \beta & 0 & 0 & 0 \\ 4\alpha X & -\beta - 3\alpha X & 2\beta b & 0 & 0 \\ 0 & 3\alpha X & -2\beta b - 2\alpha X & 3\beta b^2 & 0 \\ 0 & 0 & 2\alpha X & -3\beta b^2 - \alpha X & 4\beta b^3 \\ 0 & 0 & 0 & \alpha X & -4\beta b^3 \end{pmatrix} \mathbf{B} = \begin{pmatrix} S_0 \\ 0 \\ 0 \\ 0 \\ 0 \\ 0 \end{pmatrix},$$

where X denotes $[Ca^{2+}]_i$. α and β are rate constants for binding and unbinding of Ca^{2+} to a single Ca^{2+} binding site, and $\mathbf{B} = (B_0, B_1, B_2, B_3, B_4)$ is the vector of pool sizes of vesicles that have bound zero, one, two, three, and four Ca^{2+} ions, as denoted by the subscripts. S_0 is the total number of releasable vesicles. We also implemented cooperative Ca^{2+} binding by the factor b. Values for kinetic parameters α, β, and b were taken from Heidelberger et al. (1994). The dissociation constants for the four sequential Ca^{2+} binding steps were 143 μM, 57 μM, 23 μM, and 9 μM. The amount of transmitter release was calculated for different $[Ca^{2+}]_i$ as the equilibrium filling state of the pool B_4 ($B_4([Ca^{2+}]_i)$).

Optical setup. A monochromator-based illumination system (T.I.L.L. Photonics, Planegg, Germany) was coupled into the epifluorescence port of an inverted Axiovert 10 or IM 35 microscope (Zeiss, Oberkochem, Germany). For fluorescence measurements we used an Achrostigmat or Fluar objective (40×, 1.3 numerical aperture, oil immersion; Zeiss). Rhodamine and fura-2 were excited at 530 nm or 350/380 nm, respectively. The filter sets for rhodamine were 565DCLP, LP580 (AHF Analysentechnik, Tübingen, Germany), and those for fura-2 were DC495, LP505 (T.I.L.L. Photonics). The illumination area was reduced to a spot of ~15 μm diameter to reduce background fluorescence originating from dye-filled pipette and soma. The fluorescence detection area was adjusted by a "view finder system" (T.I.L.L. Photonics) to cover just the nerve terminal. Fluorescence light was detected with a photomultiplier tube (R928, Hamamatsu) and acquired with the Pulse software package (Heka Elektronik).

RESULTS

Loading of synprint peptide into *Xenopus* embryos

Purified synprint peptide containing the syntaxin-binding region of the N-type calcium channel was injected into one blastomere of a *Xenopus* embryo at the two- to four-cell stage. To identify peptide-containing neurons in cell culture, rhodamine-dextran was included as a fluorescent marker. After 24 hr of development (stage 19–22 according to Nieuwkoop and Faber, 1967), the spinal cord was dissected, and nerve–muscle cocultures were prepared. To determine whether injected peptide was still present and intact, we performed immunoblot analysis on pools of injected and noninjected embryos at different developmental stages. As shown in Figure 1, the peptide could still be detected in 2- and 3-d-old embryos, indicating the presence of the peptide at times when electrophysiological measurements were performed. As expected, noninjected embryos showed no immunoreactivity. The presence of the control peptide, which contained the corresponding region of an L-type calcium channel, was also confirmed by immunoblot analysis (data not shown).

Influence of synprint peptide on Ca^{2+} dependence of synaptic transmission

Assuming that the injected synprint peptide binds to syntaxin and SNAP-25 from *Xenopus*, it should exert its effect by competing with the native N-type calcium channel. Thus, the fusion machinery should be dissociated from the channel and therefore located further away from the source of Ca^{2+} influx. The uncoupled fusion complex should experience a lower calcium concentration

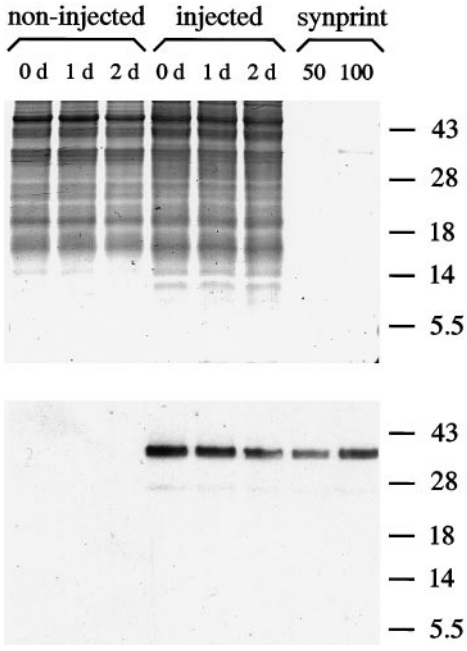

Figure 1. Presence of exogenous synprint peptide after early blastomere injection. Injected and noninjected embryos were collected at the indicated days, and the soluble fraction of one embryo was loaded into each lane. As a control, 50 and 100 ng of purified synprint peptide, respectively, were loaded into lanes 7 and 8. *Numbers on the right* indicate positions of molecular weight markers (in kDa). Two gels with identical probes were run in parallel. After SDS-PAGE, one gel was stained with Coomassie blue to demonstrate even loading (*top panel*), whereas the other was subjected to immunoblotting. Detection of synprint peptide was performed by enhanced chemoluminescence (*bottom panel*). Note the persistence of the peptide 2 d after injection, which is when all electrophysiological experiments were performed.

and have a lower release probability. To elucidate the action of the synprint peptide, we studied the effect of different external calcium concentrations ($[Ca^{2+}]_e$) on transmitter release. For these experiments nerve cells were stimulated extracellularly by a monopolar electrode to elicit action potentials, and the resulting EPSC responses were monitored on muscle cells in the whole-cell configuration. The influence of different $[Ca^{2+}]_e$ on synaptic transmission for a control cell is illustrated in Figure 2. In this experiment, a double pulse was applied every 2 sec with a 50 msec interval between the two pulses. Because of the high variability of EPSC amplitudes, at least 50 responses were averaged in each calcium concentration (Fig. 2*A*). Access resistance in the muscle cell, which was monitored continuously, was stable throughout the experiment (Fig. 2*A*, *bottom trace*). The amplitude histograms at the different external calcium concentrations showed a typical Gaussian distribution (not shown), which was taken as an indicator of a functional, mature synapse.

The double-pulse protocol also enabled us to examine the effect of external calcium concentration on paired-pulse facilitation in this preparation. This form of facilitation occurs when two stimuli are given in rapid succession and is reflected in a larger amplitude of the second EPSC, most likely attributable to elevated resting $[Ca^{2+}]_i$ remaining from the first stimulus. In Figure 2*B*, the ratios of the amplitudes of the second and first pulses are plotted against $[Ca^{2+}]_e$. Facilitation was observed in external solution containing 0.5, 1.0, and 1.8 mM calcium, being most pronounced in 0.5 mM $[Ca^{2+}]_e$ ($r = 1.47$). In 1.0 and 1.8 mM $[Ca^{2+}]_e$, the facilitation declined with ratios of 1.32 and 1.16, respectively. In 10.0 mM $[Ca^{2+}]_e$, we measured a slight depression with a ratio of 0.91, which is probably attributable to depletion of the readily releasable pool after the first stimulus. A qualitatively similar Ca^{2+} dependence of paired-pulse facilitation was observed for 25 msec pulse intervals. These data are summarized in Table 1.

An example of the dependence of the EPSC amplitude on $[Ca^{2+}]_e$ is shown in Figure 2*C*. These results show, as predicted from the classic studies on the adult neuromuscular junction, that the release is steeply dependent on $[Ca^{2+}]_e$ in the low calcium range up to 1 mM. When $[Ca^{2+}]_e$ was further elevated to 1.8 and 10.0 mM, saturation of the EPSC amplitude was observed. A slightly different dependence on the calcium concentration was found for the second EPSC, which reached its maximal amplitude at 1 mM $[Ca^{2+}]_e$. In 1.8 mM $[Ca^{2+}]_e$, the amplitude remained at the same level, whereas there was a decrease in EPSC amplitude in 10.0 mM $[Ca^{2+}]_e$.

Analysis of 14 noninjected cells illustrated that the absolute EPSC amplitudes were highly variable between cells (3.65 ± 2.45 nA for 10.0 mM $[Ca^{2+}]_e$). This variability may reflect the difference in number of terminals between each pair of cells; however, the dependence on $[Ca^{2+}]_e$ was comparable in all of these cells. Therefore, to compare between different cells, we normalized the average EPSC amplitudes to the value measured in 10.0 mM $[Ca^{2+}]_e$. On average, our experiments illustrate that for a control synapse the relative release for the first EPSCs is already close to saturation at 1.8 mM $[Ca^{2+}]_e$. Increasing the $[Ca^{2+}]_e$ by a factor of >5 (i.e., to 10.0 mM $[Ca^{2+}]_e$) caused only a 22% increase in EPSC amplitudes (see Fig. 5*B*; Table 1).

To examine the effect of the synprint peptide on transmitter release, we used either a single- or a double-pulse protocol on neuromuscular junctions, the nerve cells of which contained the synprint peptide (as identified by rhodamine fluorescence). We chose the method of early blastomere injection because large peptides are difficult to load through the recording pipette, especially when the distance between soma and terminal is highly variable (from 20 to 300 μm). A representative example of a single-pulse experiment is shown in Figure 3. In 1.8 mM $[Ca^{2+}]_e$, the average EPSC amplitude was 0.33 nA. Perfusion of the bath with 10 mM $[Ca^{2+}]_e$ caused an increase in the average EPSC amplitude to 1.1 nA. Again, perfusion with 1.8 $[Ca^{2+}]_e$ resulted in a decrease in the average EPSC amplitude to 0.51 nA, comparable to the initial value. Changing the solution into low calcium concentration (i.e., 0.5 mM $[Ca^{2+}]_e$) caused a sharp decrease to 0.2 nA and the appearance of many failures. EPSC amplitudes recovered after perfusion with 1.8 mM $[Ca^{2+}]_e$. The amplitude histogram in the different $[Ca^{2+}]_e$ showed a typical Gaussian distribution, like that of the control cell (not shown).

For comparison of the Ca^{2+} dependence of the EPSC amplitudes of peptide-injected cells with that of control cells, amplitudes were normalized to values measured in 10 mM $[Ca^{2+}]_e$ (Fig. 3*C*). When $[Ca^{2+}]_e$ is raised from 1.8 to 10.0 mM, the EPSC amplitudes increase ~2.5-fold compared with only a 1.25-fold increase in noninjected cells. An average of 19 peptide-injected cells showed that the relative release in 1.8 mM $[Ca^{2+}]_e$ was ~54% of the values obtained in 10 mM $[Ca^{2+}]_e$ (3.02 ± 2.12 nA). Double-pulse experiments with 25 msec pulse intervals indicated that the peptide had no effect on paired-pulse facilitation (Table 1).

We also performed the identical protocol on neuromuscular junctions injected with the corresponding region of an L-type calcium channel. This peptide does not bind to syntaxin or SNAP-25 in binding assays, which correlates well with the mostly postsynaptic localization of this channel (Ahlijanian et al., 1990).

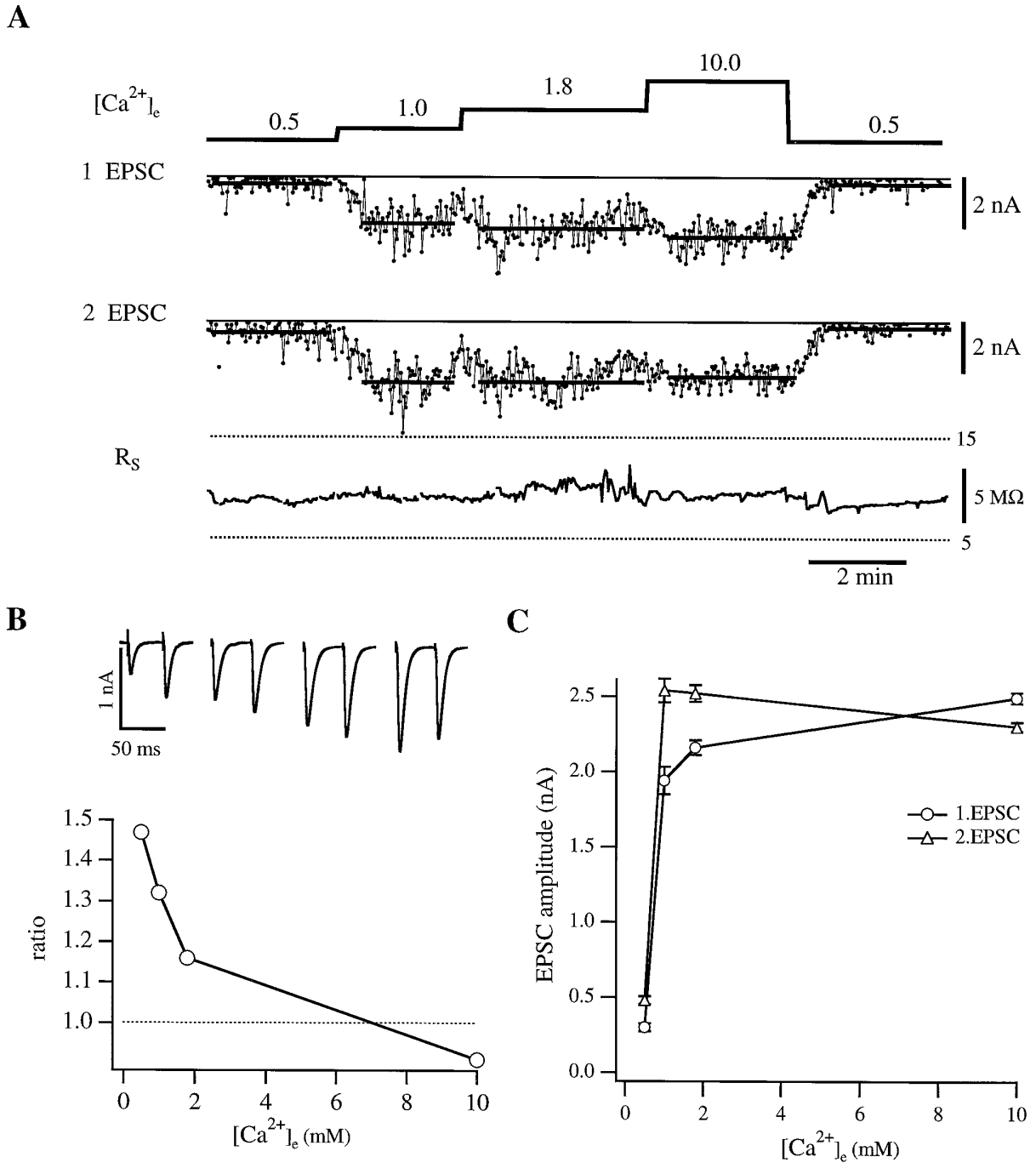

Figure 2. Representative experiment of a noninjected pair of cells with double-pulse stimulation. *A*, The *top trace* shows the different external calcium concentration $[Ca^{2+}]_e$ (in mM) during the experiment. The nerve cell was stimulated at 0.5 Hz with a pulse interval of 50 msec. In the *two middle traces* the amplitudes of the EPSCs resulting from the first and second stimulus, respectively, are displayed. The *solid lines* indicate the averaged EPSC amplitude in each $[Ca^{2+}]_e$. Because of the large variability, at least 50 responses in each $[Ca^{2+}]_e$ were averaged. The *bottom trace* shows the series resistance on the muscle cell (R_s) throughout the experiment. *B* (*top*), The average EPSCs (10 responses) in the different external calcium concentrations are displayed. $[Ca^{2+}]_e$ are 0.5, 1.0, 1.8, and 10.0 mM (*left to right*). The graph below illustrates the dependence of the ratio of 2.EPSC to 1.EPSC on the external calcium concentration. Note the constant decrease in the ratio with increasing $[Ca^{2+}]_e$. *C*, The dependence of the average EPSC amplitudes (○, 1.EPSC; △, 2.EPSC) on different $[Ca^{2+}]_e$. Error bars represent SEM.

The relative release at different external calcium concentrations in the presence of the L-type peptide was comparable to that of control cells (Table 1), indicating that the effect of the N-type synprint peptide is specific.

As shown in Figure 2*C*, the relative transmitter release in control cells increases only ~20% when the $[Ca^{2+}]_e$ was raised from 1.8 to 10.0 mM. One possible explanation for this phenomenon might be the saturation of the postsynaptic response. Therefore, we performed experiments with tetraethylammonium (TEA) and 3,4-diaminopyridine (3,4-DAP), which block voltage-gated potassium channels and consequently prolong action potentials. After application of 10–20 mM TEA and 50–100 μM 3,4-

Table 1. Summary of the Ca^{2+}-dependence of relative synaptic transmission, paired-pulse facilitation (25 msec pulse interval), and coefficient of variation

	$[Ca^{2+}]_e$ in mM			
	0.5	1.0	1.8	10.0
% Transmitter release				
Control cells	22.0 ± 5.4 (7)	52.5 ± 4.6 (8)	77.3 ± 1.8 (12)	100 (14)
Synprint (N-type)	11.6 ± 3.6 (3)	28.0 ± 3.8 (8)	53.9 ± 3.4 (17)	100 (19)
L_{II-III}670-800 (L-type)	ND	ND	69.6 ± 3.5 (14)	100 (14)
ω-conotoxin GVIA	15.5 (1)	26.0 ± 0 (2)	50.4 ± 4.5 (6)	100 (6)
Paired-pulse facilitation				
Control cells	1.60 ± 0.26 (3)	1.26 ± 0.11 (7)	1.05 ± 0.05 (5)	0.87 ± 0.06 (5)
Synprint (N-type)	ND	1.29 ± 0.09 (7)	1.06 ± 0.05 (7)	0.70 ± 0.05 (7)
L_{II-III}670-800 (L-type)	ND	1.15 ± 0.08 (5)	1.08 ± 0.09 (5)	0.72 ± 0.08 (4)
Coefficient of variation				
Control cells	0.66 ± 0.07 (8)	0.56 ± 0.11 (7)	0.40 ± 0.04 (14)	0.35 ± 0.05 (14)
Synprint (N-type)	0.67 ± 0.06 (4)	0.81 ± 0.08 (8)	0.54 ± 0.05 (17)	0.35 ± 0.03 (18)
L_{II-III}670-800 (L-type)	0.84 ± 0.29 (3)	0.67 ± 0.10 (10)	0.38 ± 0.07 (13)	0.29 ± 0.05 (13)

Data are presented for control cells (noninjected), cells injected with synprint (N-type), and control (L-type) peptides and cells treated with ω-conotoxin GVIA. Errors are given as the SEM; numbers in parentheses indicate the number of experiments. ND, Not determined.

DAP to the bath, the EPSC amplitudes in injected and noninjected cells increased up to twofold even in 10.0 mM $[Ca^{2+}]_e$, demonstrating that the postsynaptic response is not maximal under our experimental conditions (data not shown). The increase was followed by a diminishing of EPSCs attributable to blockade of acetylcholine receptors.

We also tested the possibility that the decline in relative release in control cells is attributable to saturation of the Ca^{2+} influx through the presynaptic calcium channels. Recording of single channel currents could prove this; however, because of the small size of presynaptic terminals, this is difficult to accomplish. Therefore, we used the calcium indicator dye fura-2 (Grynkiewicz et al., 1985) as a probe to measure relative Ca^{2+} influx into control terminals with 1.8 mM and 10.0 mM $[Ca^{2+}]_e$ (Neher, 1995). In addition, it remained possible that the synprint peptide exerts its effect by altering Ca^{2+} influx in 1.8 mM $[Ca^{2+}]_e$ and 10.0 mM $[Ca^{2+}]_e$. Therefore, we also measured the relative Ca^{2+} influx into peptide-loaded terminals under these $[Ca^{2+}]_e$. A representative trace of fura-2 measurements in a peptide-loaded terminal is shown in Figure 4. After whole-cell configuration on the nerve cell soma was established, 100 μM fura-2 was loaded through the pipette and allowed to equilibrate. This concentration might not fully overcome endogenous buffer, but it should yield reliable estimates of the relative Ca^{2+} influx under different external calcium concentrations. Trains of ten action potentials at a frequency of 20 Hz were given, and the resulting change of fluorescence amplitude at 380 nm was measured. The ratio of the changes in fluorescence in 10.0 and 1.8 mM external calcium $[\Delta F_{380}$ (10.0 mM)/ΔF_{380} (1.8 mM)] was 1.8 ± 0.4 (mean ± SD; n = 3) in peptide-injected terminals, whereas it was 2.0 ± 0.1 (n = 2) in control terminals. These values indicate that saturation of the Ca^{2+} influx through the presynaptic calcium channels is at least partially responsible for the saturation in relative release in high $[Ca^{2+}]_e$. They also show that the effect of the synprint peptide is not attributable to a change in relative Ca^{2+} influx at 1.8 and 10.0 mM external calcium, suggesting an action of the peptide downstream of the triggering event of synaptic transmission.

These findings suggest that the synprint peptide exerts its effect by reducing the efficiency of neurotransmitter release on the presynaptic side without affecting the Ca^{2+} influx through the channels.

Model calculations

We next tried to correlate the action of the synprint peptide with a simple model of Ca^{2+}-dependent synaptic transmission. The assumptions included in our model are illustrated in Figure 5*A*. We distinguish two classes of releasable vesicles: (*i*) vesicles linked to a Ca^{2+} channel through the synprint site and (*ii*) vesicles that are not linked to a Ca^{2+} channel. The first class senses the sum of $[Ca^{2+}]_i$ originating from Ca^{2+} influx through the local channel (termed $[Ca^{2+}]_l$) and through the channels at some distance (termed $[Ca^{2+}]_s$), whereas the second class senses only $[Ca^{2+}]_i$ from the Ca^{2+} influx through the channels at some distance. The values for "local calcium" ($[Ca^{2+}]_l$) and "surrounding calcium" ($[Ca^{2+}]_s$) are given by:

$$[Ca^{2+}]_l = a_l i([Ca^{2+}]_e)$$

$$[Ca^{2+}]_s = a_s i([Ca^{2+}]_e).$$

The factors a_l and a_s scale the relative amplitude of local and surrounding calcium, respectively. The dependence of the "relative Ca^{2+} influx" i as a function of $[Ca^{2+}]_e$ is described by $i([Ca^{2+}]_e) = [Ca^{2+}]_{i,max}/(1 + K_d/[Ca^{2+}]_e)$, with $[Ca^{2+}]_{i,max}$ = 1.0 mM. The product of $[Ca^{2+}]_{i,max} \times a_l$ determines the maximal $[Ca^{2+}]_i$ added by an open channel at infinity $[Ca^{2+}]_e$. This value scales linearly with the K_d of the secretion apparatus. From our fura-2 measurements we estimated a twofold increase of Ca^{2+} influx between 1.8 and 10.0 mM $[Ca^{2+}]_e$. Because this is a rather indirect measurement, we adapted the K_d (Ca^{2+} current) of 5.6 mM from a single channel study on L-type Ca^{2+} channels by Church and Stanley (1996). This would result in a 2.6-fold increase in Ca^{2+} influx between 1.8 and 10.0 mM $[Ca^{2+}]_e$, which is comparable to our estimates from fura-2 measurements.

If we assume further that synaptic transmission is proportional to the quadruply bound state of a calcium binding site, we can

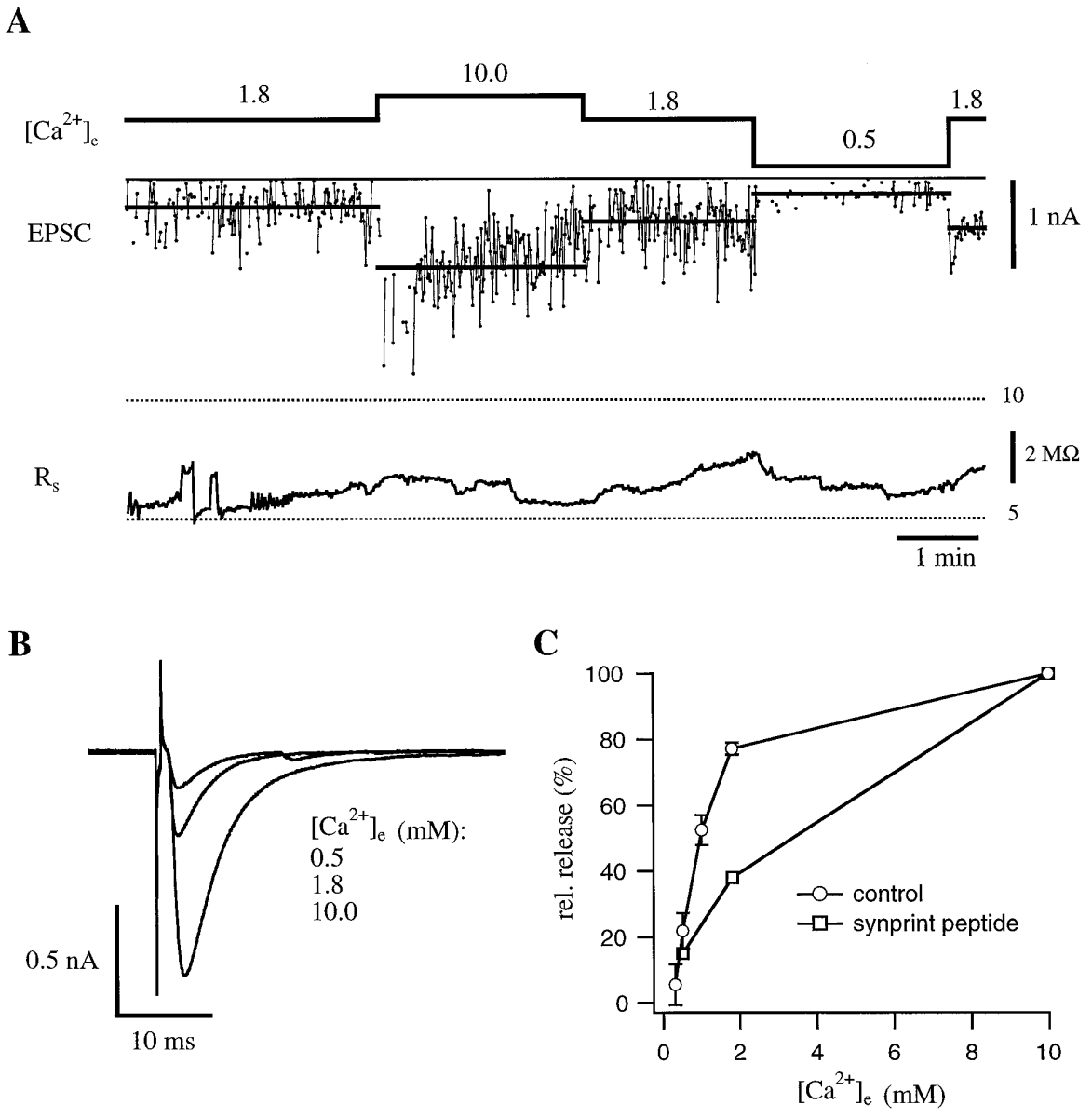

Figure 3. Representative experiment on a synapse that contained the synprint peptide. *A*, EPSCs resulting from stimulation of the nerve cell at 1 Hz. The *top trace* shows the different external calcium concentration $[Ca^{2+}]_e$ (in mM); the *bottom trace* shows the series resistance on the muscle cell (R_s) during the experiment. *B*, Examples of averaged EPSCs at the indicated external calcium concentrations. *C*, Comparison of the dependence of relative synaptic transmission on $[Ca^{2+}]_e$ for control cells and cells that contained the synprint peptide. For control cells, averaged data from 14 cells are displayed (for details, see Table 1). The curve for the synprint peptide is derived from the data shown in *A* (for averaged data of peptide-injected cells, see Fig. 5*B* and Table 1). Error bars represent SEM. Note the decrease in relative transmitter release under physiological $[Ca^{2+}]_e$ for the peptide-injected cell.

now calculate the amount of release from each class of vesicles by the following equations:

$$\text{release of linked vesicles (i)} = p_1 B_4([Ca^{2+}]_l + [Ca^{2+}]_s)$$

$$\text{release of nonlinked vesicles (ii)} = (1 - p_1) B_4([Ca^{2+}]_s),$$

with p_l denoting the probability of a docked vesicle being linked to a calcium channel.

In Figure 5*B*, a fit of our pooled experimental data for control and peptide-injected cells with the model equations is displayed. We assumed the same K_d values and cooperativity as for the goldfish bipolar terminal ($b = 0.4$) (Heidelberger et al., 1994). As mentioned above, the K_d values scale linearly with the $[Ca^{2+}]_i$. Because there are no K_d values available for this preparation, we adapted the ones measured from the bipolar nerve terminal. The sharp saturation of the dose–response curve can be influenced by both the cooperativity of the calcium binding to the secretion apparatus and the calcium dependence of the Ca^{2+} influx. Use of only one of these parameters results in rather extreme assumptions, whereas reasonable values for cooperativity ($b = 0.4$) and the calcium dependence of the Ca^{2+} influx (see above) describe our measured data well. We fixed a_l and a_s at 0.5 and 0.25, respectively, which assumes that the linked channel contributes twice as much to the local $[Ca^{2+}]$ as all the other channels together. The resulting local calcium ($[Ca^{2+}]_l$) predicted by the

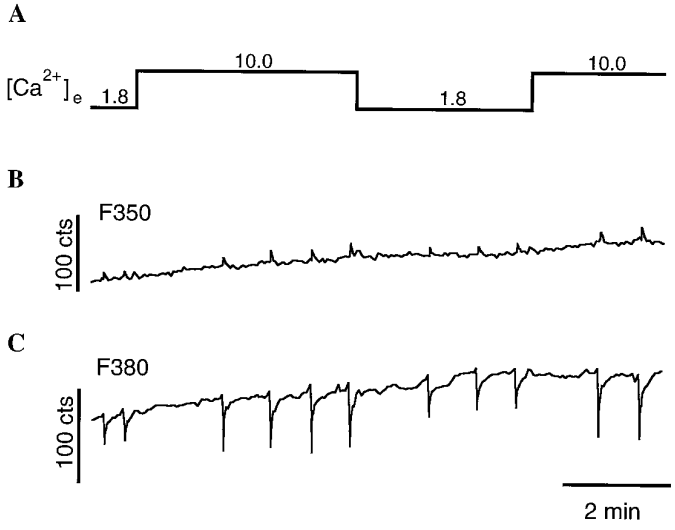

Figure 4. Measurement of the relative Ca^{2+} influx in a nerve terminal that contained the synprint peptide. Fura-2 (100 μM) was loaded through the pipette on the nerve cell soma and allowed to equilibrate. *A*, Different external calcium concentrations used during this experiment. *B, C*, Fluorescence values after excitation at 350 nm (*B, F350*) and 380 nm (*C, F380*). Shown traces start approximately 12 min after the whole-cell configuration was established on the nerve cell soma. A train of 10 action potentials was given at a frequency of 20 Hz. The relative Ca^{2+} influx was calculated from the reduction in fluorescence at 380 nm. For this experiment, the ratio of ΔF_{380} at 10 and 1.8 mM $[Ca^{2+}]_e$ was 1.8.

model is ~163 μM at 1.8 mM $[Ca^{2+}]_e$. The best fit for control cells could be obtained when 95% of the vesicles are linked to a calcium channel, which correlates well with the reported *in vivo* situation in the adult frog neuromuscular junction (Yoshikami et al., 1989). For the peptide-injected cells, the model predicts that only 25% of the vesicles remain linked to a calcium channel after action of the synprint peptide. The majority of vesicles (70%) has been uncoupled from a single calcium channel but is still releasable by increasing the Ca^{2+} influx through the channels at some distance. A major assumption of our model is the ratio of calcium concentrations sensed by linked and nonlinked vesicles. When changing this ratio from 3:1 to 5:1, the estimate for the fraction of uncoupled vesicles required for a proper fit is reduced from 70 to 60%. At the same time, however, the accuracy of the fit is reduced. These model-derived numbers may not correctly reflect the absolute numbers *in vivo*, but they indicate that in peptide-injected cells the fraction of uncoupled vesicles is larger than the measured reduction in relative release (Fig. 3*C*, Table 1). These results therefore support the conclusion that competition with the binding region on N-type channel does not prevent synaptic transmission, but it shifts its Ca^{2+} dependence to higher values.

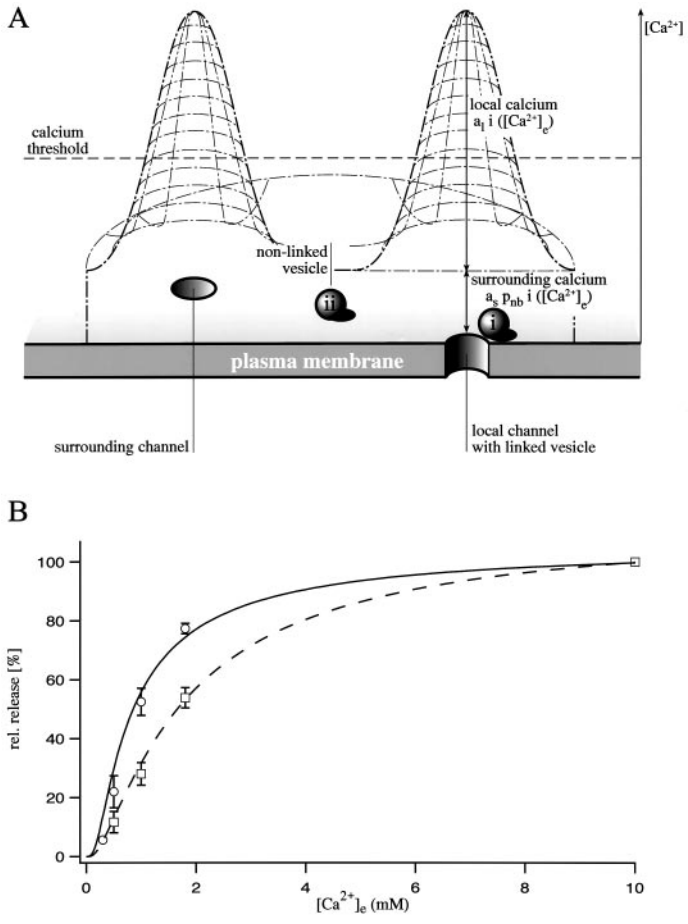

Figure 5. Correlation of the action of synprint peptide with a model of Ca^{2+}-dependent synaptic transmission. *A*, Schematic presentation of the assumptions implied in the model. The Ca^{2+} concentration at the inner surface of the membrane reaches its highest value at an open Ca^{2+} channel. With increasing distance from a channel the Ca^{2+} concentration declines, leading to the formation of so-called Ca^{2+} domains. Two classes of vesicles, linked (*i*) and nonlinked (*ii*), can be distinguished. A linked vesicle senses the sum of local and surrounding calcium, whereas a nonlinked vesicle senses just the surrounding calcium. Note that the shape of the Ca^{2+} domains is drawn schematically; for the model calculations (see Results) we assumed a cylindrical shape. Also note that the *line*, which indicates the value for the calcium threshold of synaptic transmission, should be considered arbitrary. *B*, Fit of the experimental data with model-derived curves. Pooled control data (*open circles*) are best described if one assumes that 95% of all releasable vesicles are linked to a Ca^{2+} channel (*solid curve*). For pooled data of cells containing the synprint peptide (*open squares*), the model predicts that only 25% of all releasable vesicles remained linked to a Ca^{2+} channel (*dashed curve*). Error bars represent SEM.

Mimicking the synprint peptide effect with ω-conotoxin GVIA

An alternative approach that should mimic the action of the synprint peptide is the irreversible blockade of a portion of the calcium channels involved in transmitter release by toxin. In terms of our model described above, blocking channels will have two effects. (1) The fraction of blocked channels will no longer contribute to the Ca^{2+} influx. This leads to a reduction in surrounding calcium concentration. (2) A vesicle that is linked to a blocked Ca^{2+} channel will be converted to the class of nonlinked vesicles experiencing only the surrounding calcium.

A vesicle linked to a blocked channel will not be released, if we assume that the surrounding calcium concentration is below the threshold to stimulate release (Fig. 6, *bottom left panel*). Increasing calcium influx through the neighboring channels by elevating $[Ca^{2+}]_e$ (i.e., from 1.8 to 10.0 mM), however, will lead to a rise in calcium in the vicinity of this vesicle and therefore increase its probability of release (Fig. 6, *bottom right panel*). We used the following experimental approach to examine this question. ω-conotoxin GVIA (200 nM), an irreversible blocker of the N-type calcium channel, was applied to the bath, and EPSCs were monitored before and after toxin application. EPSCs were evoked every 2 sec as described for Figures 2 and 3. Shortly after application of the toxin, EPSC amplitudes started to decline from

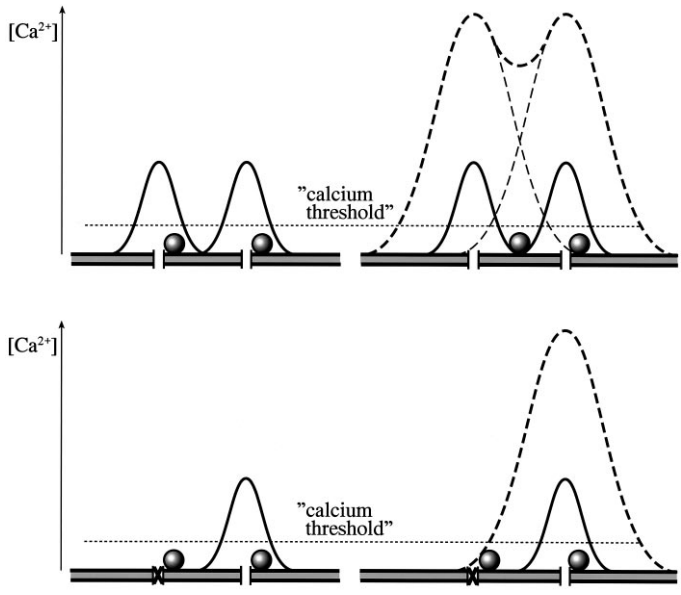

Figure 6. Schematic comparison of actions of the synprint peptide and an irreversible Ca^{2+} channel blocker. The *top panel* illustrates the proposed action of the synprint peptide, starting from the situation in the uninjected neuromuscular junction where both shown vesicles are linked to a certain Ca^{2+} channel (*left*). The *solid lines* represent the Ca^{2+} domains in 1.8 mM $[Ca^{2+}]_e$; the *horizontal, dotted line* indicates an assumed calcium threshold. After opening of the Ca^{2+} channels, both vesicles would be released. After action of the synprint peptide (*right*), a vesicle was uncoupled from a Ca^{2+} channel. In 1.8 mM $[Ca^{2+}]_e$, only one vesicle would be released, resulting in a reduction of EPSC amplitude. Rising $[Ca^{2+}]_e$ from 1.8 to 10.0 mM (*dashed lines*), however, would release both vesicles. In the *bottom panel*, the action of an irreversible Ca^{2+} channel blocker, e.g., ω-conotoxin GVIA, is illustrated. In the situation on the *left*, the toxin has blocked one of the Ca^{2+} channels. EPSC amplitude would be reduced in 1.8 mM $[Ca^{2+}]_e$ (*solid lines*), because the linked vesicle at the blocked channel would not be released. Rising $[Ca^{2+}]_e$ from 1.8 to 10.0 mM (*dashed lines*) would again release both vesicles because of the increased Ca^{2+} domain of the open Ca^{2+} channel.

6 to <1 nA (Fig. 7*A*). Thereafter, excess toxin was removed by perfusion for 2 min in 10 mM $[Ca^{2+}]_e$, which led to an increase in average EPSC amplitude to 1.7 nA. After perfusion with 1.8 mM $[Ca^{2+}]_e$, EPSCs decreased to 0.86 nA, a reduction to <60% of the average amplitude recorded in 10 mM $[Ca^{2+}]_e$. Perfusing again with 10 mM $[Ca^{2+}]_e$ resulted in an increase of the average amplitude to 2.5 nA. Lowering the external calcium to 0.3 mM caused a remarkable decrease in the amplitude to <0.2 nA, which corresponds to <20% of the average amplitude recorded in 10 mM $[Ca^{2+}]_e$. The pooled data for the toxin experiments are shown in Table 1; the average amplitude in 10 mM $[Ca^{2+}]_e$ was 1.55 ± 0.36 nA.

Comparison of the relative amplitudes in the toxin experiment with those of the control cells reveals that the dependence on external calcium is very different (Fig. 7*C*). On the other hand, the toxin curve is very similar to the one obtained in peptide-loaded neurons, showing a higher dependence of synaptic transmission on external calcium. It also correlates well with the assumption that transmitter release in the case of blocked channels could be partially restored by increasing $[Ca^{2+}]_e$ from 1.8 to 10.0 mM. It is difficult, however, to calculate the percentage of blocked channels from the relative decrease in release, because the relation between calcium concentration and release is not linear. To use our model to estimate the portion of blocked channels, we introduced p_{nb} as the probability of a channel not being blocked. Although the value for local calcium ($[Ca^{2+}]_l$) would not be influenced, that of surrounding calcium ($[Ca^{2+}]_s$) would then be given by:

$$[Ca^{2+}]_s = a_s p_{nb} i([Ca^{2+}]_e).$$

The amount of release for each class of vesicles would then be calculated with the following equations:

$$\text{release of linked vesicles (i)} = p_1 p_{nb} B_4([Ca^{2+}]_l + [Ca^{2+}]_s)$$

$$\text{release of nonlinked vesicles (ii)} = (1 - p_1 p_{nb}) B_4([Ca^{2+}]_s).$$

For the toxin simulation we used the same assumptions as for the control cells (95% of the vesicles are docked, and the ratio between local calcium and surrounding calcium is 3:1). According to the simulation, block of 60% of the channels would account for an expected inhibition of 80% in relative transmitter release (Fig. 7*C*).

Thus, the experimental data as well as our model calculations suggest that uncoupling a vesicle from the calcium channel through the action of the synprint peptide or alternatively blocking a fraction of the channels irreversibly will lead to a similar change in the calcium dependence of synaptic transmission.

DISCUSSION

We have demonstrated that injection of peptides containing the soluble NSF attachment protein receptor (SNARE) protein-binding region of N-type Ca^{2+}-channels changes the Ca^{2+}-dependence of transmitter release in cultured frog neuromuscular junctions. This effect is most pronounced under physiological conditions, i.e., in external solution containing 1.8 mM calcium. Our findings support the *in vitro* binding data (Sheng et al., 1994), which revealed an interaction of the N-type but not the L-type calcium channel with syntaxin and SNAP-25 through that synprint site. They are also consistent with the data on rat superior cervical ganglion neurons (Mochida et al., 1996), in which a maximum of 42% inhibition of synaptic transmission was observed after diffusion of synprint peptide.

Our results further show that the effect of the synprint peptide is attributable to neither reduced relative Ca^{2+} influx into the terminal nor saturation of the postsynaptic response. It has been reported that coexpression of syntaxin with L-, Q- and N-type calcium channels in *Xenopus* oocytes resulted in a decrease of calcium influx through these channels because of stabilization of the inactivated state (Bezprozvanny et al., 1995; Wiser et al., 1996), but this effect was not observed in isolated chick ciliary ganglion nerve terminals (Stanley and Mirotznik, 1997). If syntaxin inhibits Ca^{2+} channel function in our preparation, disruption of the native syntaxin/channel-interaction by the synprint peptide would therefore lead to an increase in Ca^{2+} influx and consequently to an underestimation of the physiological effect. Our fura-2 measurements indicate that the ratio of relative Ca^{2+} influx into injected and control terminals at 1.8 and 10.0 mM external calcium is virtually identical (see Results). Because we do not measure the absolute Ca^{2+} influx at a given calcium concentration, an equal increase in influx into injected terminals in both 1.8 and 10.0 mM $[Ca^{2+}]_e$ still remains possible.

The model calculations in Figure 5 suggest that the observed 25% reduction in relative release in 1.8 mM external calcium corresponds to an uncoupling of ~70% of the formerly linked vesicles by the synprint peptide. The fast, Ca^{2+}-dependent synaptic transmission at this neuromuscular junction is entirely blocked by application of the N-type-specific ω-conotoxin GVIA (Yazejian et al., 1997), but the toxin blocks Ca^{2+} influx and

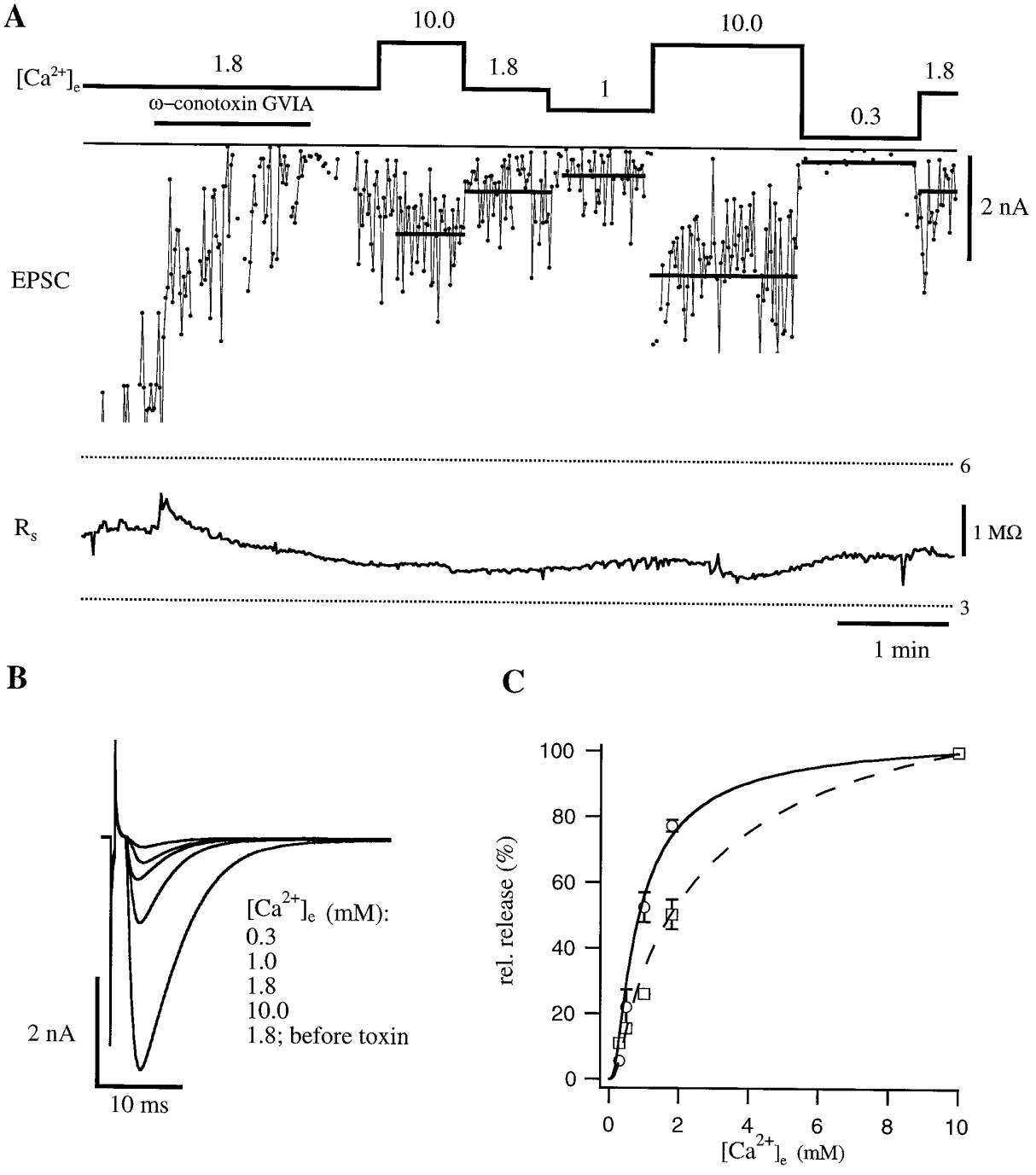

Figure 7. Ca^{2+} dependence of EPSC amplitudes after blockade of a fraction of Ca^{2+} channels by ω-conotoxin GVIA. *A*, EPSCs resulting from stimulation of the nerve cell at 0.5 Hz. ω-conotoxin GVIA (200 nM) was applied (indicated by the *bar*), leading to a decrease in EPSC amplitude. After washout of the toxin, a stable fraction of Ca^{2+} channels remained blocked. The *top trace* shows the different external calcium concentration $[Ca^{2+}]_e$ (in mM); the *bottom trace* shows the series resistance on the muscle cell (R_s) during the experiment. *B*, Examples of averaged EPSCs at the indicated external calcium concentrations. Note that the shape of EPSCs remained unaltered by the blockade of Ca^{2+} channels. *C*, Comparison of the dependence of relative transmitter release on $[Ca^{2+}]_e$ for control synapses and synapses that had been treated with ω-conotoxin GVIA. For both types of synapses, averaged data of different cells are displayed (for details, see Table 1). Pooled control data (*open circles*) are best described if one assumes that 95% of all releasable vesicles are linked to a Ca^{2+} channel (*solid curve*). The Ca^{2+} dependence of synapses treated with ω-conotoxin GVIA (*open squares*) is predicted by the model, if it is assumed that 60% of the Ca^{2+} channels have been blocked (*dashed curve*). Error bars represent SEM.

increases the number of vesicles linked to blocked channels, so it reduces Ca^{2+} at both coupled and uncoupled vesicles. One possible explanation for the vesicle fraction remaining linked to a calcium channel would be the incomplete action of the synprint peptide. We consider this possibility not very likely, because varying the amount of injected peptide over a wide range did not markedly change the effect, suggesting that the peptide was already present in excess. Rather, the vesicle fraction remaining linked to a calcium channel might be attributable to the high density of calcium channels in the active zones of the frog neu-

romuscular junction (Heuser and Reese, 1981; Robitaille et al., 1990). The effect of moving vesicles away from local channels would then reach a maximum of reduction in transmitter release, after which the Ca^{2+} influx through surrounding channels is high enough to exceed the threshold of release.

Our model calculations also provide an explanation for the already high relative transmission of control cells in 1.8 mM external calcium concentration. If indeed almost all vesicles are linked to a local channel in this preparation, only minimal Ca^{2+} influx is needed to release them. The short distance between the channel as the Ca^{2+} source and the Ca^{2+} sensor of release would give endogenous calcium buffers little time to remove the high calcium at the inner mouth of the channel and consequently increase the probability of transmitter release. This assumption is supported by biochemical data that identified the Ca^{2+} binding protein synaptotagmin as an integral member of the SNARE-complex (for review, see Südhof, 1995).

In conclusion, our data further underscore the physiological importance of the interaction between presynaptic Ca^{2+} channels and members of the docking and fusion machinery. Interruption of this physical link does not prevent synaptic transmission, but makes it less probable by shifting its Ca^{2+} dependence to higher values.

REFERENCES

Ahlijanian MK, Westenbroek RE, Catterall WA (1990) Subunit structure and localization of dihydropyridine-sensitive calcium channels in mammalian brain, spinal cord, and retina. Neuron 4:819–832.

Bennett MK, Calakos N, Scheller RH (1992) Syntaxin: a synaptic protein implicated in docking of synaptic vesicles at presynaptic active zones. Science 257:255–259.

Bezprozvanny I, Scheller RH, Tsien RW (1995) Functional impact of syntaxin on gating of N-type and Q-type calcium channels. Nature 378:623–626.

Borst JGG, Sakmann B (1996) Calcium influx and transmitter release in a fast CNS synapse. Nature 383:431–434.

Burgoyne RD, Morgan A (1995) Ca^{2+} and secretory-vesicle dynamics. Trends Neurosci 18:191–196.

Church PJ, Stanley EF (1996) Single L-type calcium channel conductance with physiological levels of calcium in chick ciliary ganglion neurons. J Physiol (Lond) 496:59–68.

Dodge FA, Rahamimoff R (1967) Cooperative action of calcium ions in transmitter release at the neuromuscular junction. J Physiol (Lond) 193:419–432.

Fatt P, Katz B (1951) An analysis of the end-plate potential recorded with an intracellular electrode. J Physiol (Lond) 115:320–370.

Grynkiewicz G, Poenie M, Tsien RY (1985) A new generation of Ca^{2+} indicators with greatly improved fluorescent properties. J Biol Chem 260:3440–3450.

Heidelberger R, Heinemann C, Neher E, Matthews G (1994) Calcium dependence of the rate of exocytosis in a synaptic terminal. Nature 371:513–515.

Heinemann C, Chow RH, Neher E, Zucker RS (1994) Kinetics of the secretory response in bovine chromaffin cells following flash photolysis of caged Ca^{2+}. Biophys J 67:2546–2557.

Heuser JE, Reese TS (1981) Structural changes after transmitter release at the frog neuromuscular junction. J Cell Biol 88:564–580.

Llinas RR, Steinberg IZ, Walton K (1981) Relationship between presynaptic calcium current and postsynaptic potential in squid giant synapse. Biophys J 33:323–351.

Mochida S, Sheng Z-H, Baker C, Kobayashi H, Catterall WA (1996) Inhibition of neurotransmission by peptides containing the synaptic protein interaction site of N-type Ca^{2+} channels. Neuron 17:781–788.

Neher E (1995) The use of fura-2 for estimating Ca buffers and Ca fluxes. Neuropharmacology 34:1423–1442.

Nieuwkoop PD, Faber J (1967) Normal table of *Xenopus laevis*, second edition. Amsterdam: North Holland.

Oyler GA, Higgins GA, Hart RA, Battenberg E, Billingsley M, Bloom FE, Wilson MC (1989) The identification of a novel synaptosomal associated protein, SNAP-25, differentially expressed by neuronal subpopulations. J Cell Biol 109:3039–3052.

Robitaille R, Adler EM, Charlton MP (1990) Strategic location of calcium channels at transmitter release sites of frog neuromuscular synapses. Neuron 5:773–779.

Sheng Z-H, Rettig J, Takahashi M, Catterall WA (1994) Identification of a syntaxin-binding site on N-type calcium channels. Neuron 13:1303–1313.

Sheng Z-H, Rettig J, Cook T, Catterall WA (1996) Calcium-dependent interaction of N-type calcium channels with the synaptic core complex. Nature 379:451–454.

Stanley EF, Mirotznik RR (1997) Cleavage of syntaxin prevents G-protein regulation of presynaptic calcium channels. Nature 385:340–343.

Südhof TC (1995) The synaptic vesicle cycle: a cascade of protein-protein interactions. Nature 375:645–653.

Tabti N, Poo M-M (1991) Culturing spinal neurons and muscle cells from *Xenopus* embryos. In: Culturing nerve cells (Banker G, Goslin K, eds), pp 137–154. Cambridge, MA: MIT.

Wiser O, Bennett MK, Atlas D (1996) Functional interaction of syntaxin and SNAP-25 with voltage-sensitive L- and N-type Ca^{2+} channels. EMBO J 15:4100–4110.

Yazejian B, DiGregorio DA, Vergara JL, Poage RE, Meriney SD, Grinnell AD (1997) Direct measurements of presynaptic calcium and calcium-dependent potassium currents regulating neurotransmitter release at cultured *Xenopus* nerve-muscle synapses. J Neurosci 17:2990–3001.

Yoshida A, Oho C, Omori A, Kuwahara R, Ito T, Takahashi M (1992) HPC-1 is associated with synaptotagmin and ω-conotoxin receptor. J Biol Chem 267:24925–24928.

Yoshikami D, Bagabaldo Z, Olivera BM (1989) The inhibitory effects of omega-conotoxins on Ca channels and synapses. Ann NY Acad Sci 560:230–248.